FOREX Publication
Open Access | Rapid and quality publishing

International Journal of
Electrical and Electronics Research (IJEER)
Research Article | Volume 11, Issue 2 | Pages 457-464 | e-ISSN: 2347-470X

Development and Application of an Energy Management System for Electric Vehicles Integrated with Multi-input DC-DC Bidirectional Buck-Boost Converter

Jarapala Ramesh Babu[1*], Manas Ranjan Nayak[2] and B.Mangu[3]

[1,2]Department of Electrical Engineering, Biju Patnaik University of Technology Rourkela, Odisha, 769015, India, babu.ramesh444@gmail.com[1], manasnk72@gmail.com[2]
[3]Department of Electrical Engineering, University college of Engineering, Osmania University, Hyderabad, 500007, India, bmanguou@gmail.com[3]

***Correspondence:** Jarapala Ramesh Babu, Email: babu.ramesh444@gmail.com

ABSTRACT- The rise in environmental pollution, demand for fossil fuels, and higher fuel economy vehicles has raised concerns about the creation of new and efficient transportation vehicles in recent days. These days, most developments in electric vehicles concentrate on making the vehicles more pleasant to ride in. Nonetheless, the emphasis now should be on energy and its most efficient use. To do this, you must give your attention to the origin of the automobile. The answer to this problem may be found in hybrid energy storage systems (HESS). This work is concerned with the design and implementation of an effective energy management system in electric vehicles (EVs) equipped with an active HESS consisting of a battery and a super capacitor via the incorporation of load sharing into this hybridization under a variety of load demand scenarios. To address the demands of high fuel efficiency vehicles, automotive firms are focusing on the development of diesel-engine operated vehicles, electric vehicles, fuel-cell vehicles, plug-in electric vehicles, and hybrid electric vehicles. A Multi-input Bidirectional Buck-Boost (MIB[3]) DC-DC converter is proposed in this dissertation to provide a greater conversion ratio to the input DC voltage. The multi-input converter recommended has fewer components and a simpler control method, making it more trustworthy and cost-effective. This converter also has bidirectional power flow functionality, making it suitable for charging the battery during regenerative braking in an electric or hybrid vehicle. Three different energy sources are used in the suggested topology: a photovoltaic (PV) panel, a battery, and an ultra-capacitor.

Keywords: Multi-input dc-dc converter, Hybrid energy storage system (HESS), ultra-capacitor (UC), BLDC motor.

ARTICLE INFORMATION

Author(s): Jarapala Ramesh Babu, Manas Ranjan Nayak and B.Mangu;

Received: 18/2/2023; **Accepted**: 13/06/2023; **Published**: 30/06/2023;
E- ISSN: 2347-470X;
Paper Id: IJEER230207;
Citation: 10.37391/IJEER.110228
Webpage-link:
https://ijeer.forexjournal.co.in/archive/volume-11/ijeer-110228.html

1. INTRODUCTION

The main drawbacks of internal combustion engine-powered autos are rising fuel costs, pollution issues, and fossil fuel depletion. To address the aforementioned challenges, the automobile industry has begun to demonstrate an interest in vehicles that use alternative energy sources. As a result, electric vehicles (EVs) and plug-in hybrid EVs are becoming increasingly popular. Thus, energy storage equipment such as batteries and ultra-capacitors can be used to convert traditional vehicular systems into electric or hybrid electric vehicle.

Concerns about environmental degradation have raised demand for non-polluting and energy-efficient automobiles (Shiue & Lin 2011, Wyczalek 1995, Rajashekara & Martin 1995, Yang et al. 2002, Shiue & Lin 2011). Because of the growing demand for non-polluting vehicles, the automotive industry is concentrating on the development of electric vehicles (EV), fuel cell vehicles (FCV), plug-in hybrid electric vehicles (PHEV), PV interfaced electric vehicles, and hybrid electric vehicles (HEV) (Emadi et al. 2008, Daya et al. 2016, Kim 2011). Among these, electric vehicles (EVs) and hybrid electric vehicles (HEVs) offer a viable solution for reducing CO2 emissions and fossil fuel consumption (Gao et al. 2007, Chau et al. 2008, Miet al. 2005). During acceleration, the EV and HEV use electrical energy to complement the output of an internal combustion (IC) engine, and during braking, the energy supplied by the electric motor is restored[1] [2] [3] [4].

The following criteria define the EV and HEV's capability: 1) the ability to reduce the battery storage unit's power consumption during acceleration. 2) The system's ability to recover electrical energy lost during braking. 3) the ability to eliminate the IC Engine's perfect operation, and 4) the capacity to produce enough torque to fulfil demand. Researchers have come up with a lot of different ways to make HEVs and EVs more efficient and cheaper. Xiong et al. (2008), Chan 2007, and Rajashekara (2013) are some of them[5].
To govern the power flow from car to home and home to vehicle, the smart controller has been connected to the status of

FOREX Publication
Open Access | Rapid and quality publishing
International Journal of Electrical and Electronics Research (IJEER)
Research Article | Volume 11, Issue 2 | Pages 457-464 | e-ISSN: 2347-470X

charge. The design of a parallel resonant LC converter for transporting PV power in electric vehicles has been proposed (Slah et al. 2018). To ensure great efficiency during the conversion, the converter is built with a planar transformer, two complete bridges, and LC resonant filters. Compared to other converter topologies, coupled inductor-based converters are more efficient, according to a study of existing converter topologies[6].

This study presents the design and implementation of a modular four-port bidirectional buck-boost converter for integrating many energy sources, including batteries, ultra-capacitors, and solar panels. Once the bidirectional converter's output is fed into the three-phase inverter, the dc power is converted to ac, and an LC filter is used to get a smooth sinusoidal curve, allowing a traction motor to operate at constant speeds with no distortion. The separate converter may use either a parallel or series connection to the energy source. For a series connection to work, all of the conductors must be able to carry the same current, and a parallel converter must provide the same voltage across all of the connections. Both of these are quite undesirable. Multi-input, single-output (MISO) systems, however, are commendable due to their low cost and excellent efficiency[7] [8] [9]. The proposed converter has many operating modes, including single input, dual output (SIDO), dual input, single output (DISO), and even single input, tri output (SITO).

These research gaps are addressed in this study by providing the following contributions:

(1) Developing a multi-input converter architecture and controller for use in the design of an EV powertrain that incorporates BU-UC as hybrid sources including precise switching patterns for driving and regenerative braking mode was a priority for the designers.

(2) Use the transfer function model to make a precise buck-boost bidirectional DC-DC converter controller that is not inverted [10] [11].

(3) Implements an adaptive EMS that places a premium on the dynamic properties of hybrid sources in order to control energy consumption.

(4) Two different types of energy storage technologies, including a battery and an ultra-capacitor, are used to provide reliable power to HEVs [12].

(5) In this situation, the HEV receives its effective power, and the suggested solution increases the motor and vehicle's speed while simultaneously enhancing their torque output. Power may be transferred from a variety of sources to a load, and it does so efficiently and effectively [13] [14] [15] [16]. The converter's compact design and reduced component count improve its dependability, Proposed Multi-input Bidirectional Buck-Boost DC-DC Converter for electric vehicle as shown in *figure 1* and Appraisal Table of Proposed Multi-input Bidirectional Buck-Boost DC-DC Converter (MIB^{3}DC-DCC) in *table 1*.

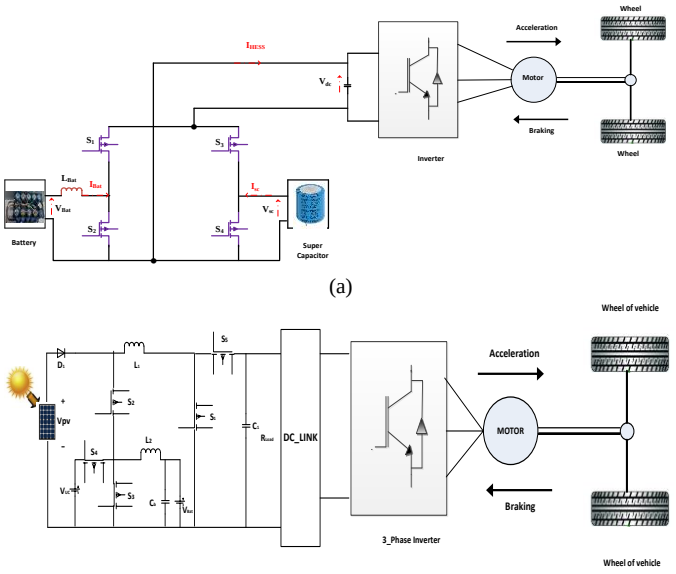

Fig.1. (a) Block diagram of the proposed system of battery and Super-capacitor. (b)Proposed Multi-input Bidirectional Buck-Boost DC-DC Converter for electric vehicle.

Table 1. Appraisal Table of Proposed Multi-input Bidirectional Buck-Boost DC-DC Converter (MIB^{3}DC-DCC)

Topology of the converters	Number of inputs	Number of output	Number of inductors	Number of switches	Number of diodes	Number of capacitors
1. Consider conventional one boost converter and two bidirectional buck boost converter.	3	1	3	5	1	1
2. Comparative analysis of bidirectional 3level dc-dc converter for automotive applications.	1	1	1	4	-	1
3. A bidirectional no isolated multi-input dc-dc converter for hybrid energy storage system in electric vehicle.	3	1	3	5	3	1
4. A novel step-up multi-input dc-dc converter for hybrid electric vehicle application.	3	1	2	4	5	2
5. A new three input dc/dc converter for hybrid pv/fc/battery application.	3	1	2	4	4	2
6. Modular multi-input bidirectional dc to dc converter for multi-source hybrid electric vehicle application.	3 or 1	3 or 1	2	5	1	2
Proposed converter (MIB^{3}DC-DCC)	**3 or 1**	**1 or 3**	**2**	**7**	**5**	**4**

FOREX Publication
Open Access | Rapid and quality publishing
International Journal of Electrical and Electronics Research (IJEER)
Research Article | Volume 11, Issue 2 | Pages 457-464 | e-ISSN: 2347-470X

The last portion of the paper presents the findings and discussion of the study.

1.1 Statement of the Problem

1.1.1. It is urgently necessary to create a sustainable and affordable method of storing energy from a wide range of sources.

1.1.2. Batteries very rarely start off at zero voltage, and even if they do, a relatively tiny charge is all that's needed to get them to a significant proportion of the open-circuit voltage.

1.1.3. This article investigates the EV's load requirements, but only for the propulsion load type. Despite the fact that the analysis considers non-propulsion load requirements.

2. PROPOSED PV-DHEV CONFIGURATION

Figure 1, depicts the power circuit topology of the proposed PV interfaced multi-input bidirectional buck-boost DC-DC converter driven Drive Hybrid Electric Vehicle (DHEV). The suggested system has less switches and power conversion stages than other systems. The PV array coupled to the inductors L_1 and L_2 provides a first stage of voltage boosting to the PV array's voltage. Connecting a high-frequency (HF) boosting transformer to the three-port converter improves its boosting potential even more. The isolation between the DC link and the PV arrays is also provided by the HF transformer. Bidirectional control of power transmission from battery to DC link and vice versa is provided via a bidirectional buck-boost DC-DC converter connected to the DC connection. The bidirectional converter can also be used to harness power from the PMSM motor by connecting diodes in parallel with the inverter's MOSFET. The suggested converter topology maintains a constant current between the DC link and the PV array. During the next sections, we show the steady state analysis of the proposed PV-DHEV in both acceleration and deceleration modes.

2.1 Multi-input Topology Operation

A PV panel, a battery backup, an ultra-capacitor, and a DC/DC multi-input converter with a power inverter are shown in the functional diagram of an electric vehicle system (*See fig.1*). system of propulsion. The input PV source is connected across in this case. The output of the proposed multiport converter is connected to the vehicle's drive train, which is connected to the converter. An ultra-capacitor can be built inside the battery unit. Increase the amount of output. Two inductors L_1 & L_2, two capacitors C_1 & C_b, five active switches S_1, S_2, S_3, S_4, S_5, and one diode make up the DC-DC bidirectional converter (*See fig. 1*) The duty cycles for switches S_1, S_2, S_3, S_5, and S_4 are set correctly (d_1, d_2, d_3, d_{11}, d_{22}). The suggested universal DC-DC converter is a MIB^{3}C (multi-input bidirectional buck-boost converter), with PV as the primary generation unit and the battery and ultra-capacitor as the secondary storage units. The circuit's storage units can store regenerative energy and deliver additional energy during acceleration.

In continuous conduction mode (CCM), MIB3C functions in four different ways (*See fig. 1*):

Case 1: The power is transferred between the source and the load using V_{PV} or V_{DC} (ultra-capacitor and battery charge).
Battery ($V_{Battery}$) to load (battery acquittals and ultra-capacitor charges).
Case II: Ultra-capacitor ($V_{U\text{-}C}$) to load (battery charges and ultra-capacitor acquittals).
Case III: The ultra-capacitor and battery are powered by regenerative power (ultra-capacitor and battery in charging action).

2.1.1 CASE-I: PV-Voltage ⟶ ($V_{battery}$ and $V_{U\text{-}C}$ (Buck), V_{output}(Boost)

In this case, the converter operates in two modes, with diode D_1 always on.
Mode of Operation-I: S_1, S_2, S_4, and D_1 are switched on, but S_5, S_3, and D_1 are turned off. As a result, both inductors L_1 and L_2 are powered in order to supply PV power to the load. The battery charges in this mode *(See fig. 2 (a)).*

Mode of Operation-II: Switches S_1 and S_2 are switched off in this mode. The S_3, S_5, and S_4 have been activated. As a result, L_1 releases the increased output into the stream. The battery is continually charged via the inductor L_2 during this period (*See fig. 2 (b)).* As a result, the converter gives off buck output at the same time across the battery in this case.

2.1.1.1 Continuous Conduction Modes Derivation (CCM)

2.1.1.1.1. Ideal multi-input bidirectional converter in order to look into the converter case-1 steady state in CCM, the parasitic performance (*See table 2*) Inductor resistance, switch resistance, and other parameters such as the voltage drop in the switches (S_1 in d1 duty cycle), and diodes are regarded as insignificant. Employing the converter delivers a boosted output and is derived from the voltage-second balance idea for modes (I) and (II). As a result of the capacitor C_1

$$V_{dc-pv} = \frac{V_{dc}}{(1-d_1)} \quad (1)$$

Where $V_{dc\text{-}pv}$ is input PV voltage, V_{L1} is the inductor L_1 voltage. After Switch S_2 is ON, the battery voltage can be derived as

$$V_{Batt} = d_2 V_{pv} \quad (2)$$

$$V_{U-C} = d_2 V_{pv} \quad (3)$$

Where V_{Bat} denotes the voltage of the battery, as a result, the voltage change in the battery is given by

$$\Delta V_{output} = -\frac{I_o d_1}{C_1 F_{sy}} (4)$$

$$\Delta V_{Batt} = -\frac{I_{ob} d_2}{C_{batt} F_{sy}} \quad (5)$$

In the case of ultra-capacitors, it's the same way

$$\Delta V_{U-C} = -\frac{I_o d_2}{F_{sy}} \quad (6)$$

2.1.1.1.2 Non-deal MIB^{3}C the non-ideal activities of the converter can be defined as follows when parasitic parameters are incorporated into the converter elements. The entire power while boosting can be written as

FOREX Publication
Open Access | Rapid and quality publishing
International Journal of Electrical and Electronics Research (IJEER)
Research Article | Volume 11, Issue 2 | Pages 457-464 | e-ISSN: 2347-470X

$V_{pv}.I_{pv}=V_oI_o+P_{rL}+P_{sw}+P_{D1}$

$$V_{pv}I_{pv} = V_{dc-pv}I_0 + r_{L2}{I_{L2}}^2 + d_1 r_{sw1}{I_{L1}}^2 + 0.5C_{sw1}{V_{sw1}}^2 f_{sy} + (1-d_1)Vd_2I_{L2} \quad (7)$$

The losses across the diodes, inductor, and switches are represented by P_{D1}, P_{rL}, and P_{SW}, respectively. The current load can now be written as

$$I_{L1} = \frac{I_0}{(1-d_1)} \quad (8)$$

As a result, the converter's output is enhanced

$$V_{dc-pv} = V_{pv}I_{pv} + (d_1-1)*\left\{\frac{1}{(1-d_1)} + \frac{R(1-d_1)}{r_{L1}} + \frac{R(1-d_1)}{d_1 r_{L1}} + \frac{2}{(1-d_1)RC_{sw1}{V_{sw1}}^2 F_{sy}}\right\} \quad (9)$$

In the same way, the non-ideal buck output may be calculated as

$$V_{pv}I_{pv} = V_{Batt}I_{Batt} + r_{L2}{I_{L2}}^2 + d_2 r_{sw2}{I_{L2}}^2 + 0.5C_{sw2}{V_{sw2}}^2 f_{sy} + Vd_1I_{L2} \quad (10)$$

When the PV source charges the battery during buck operation, the battery charging current, (I_{batt}), is calculated

$$I_{L2}=\frac{I_{Batt}}{(1-d_2)} \quad (11)$$

As a result, the charging voltage of the battery can be written as

$$-V_{D1}\left\{\frac{1}{(1-d_1)} + \frac{r_i(1-d_2)}{r_{L2}} + \frac{r_i(1-d_2)}{d_2 r_{sw2}} + \frac{2}{C_{sw2}{V_{sw2}}^2 F_{sy}(1-d_1)r_i}\right\} \quad (12)$$

$$V_{U-C} = V_{pv}I_{pv} - V_{D2}\left\{\frac{1}{(1-d_2)} + \frac{r_i(1-d_2)}{r_{L2}} + \frac{r_i(1-d_2)}{d_2 r_{sw2}} + \frac{2}{{V_{sw2}}^2 F_{sy}(1-d_2)r_i}\right\} \quad (13)$$

2.1.2 CASE-II: $V_{Battery} \longrightarrow$ (V_{U-C} (Boost) and V_o (Buck), V_{output}(Boost)

Mode of Operation-III: Switches S_1, S_2, and S_3 are turned on in this mode, while S_5 and S_4 are turned off. As a result, inductor L_1 and L_2 are powered by the battery (*See fig. 2 (c)).*

Mode of Operation-IV: When the switches S_1 and S_3 are turned off, the switches S_2, S_5, and S_4 are switched on. As a result, inductors L_1, L_2, and the battery are discharged via switches S_4 and S_5. (*See fig. 2 (d)* for more information.) Because L_1 and L_2 are in series with the load, inductor current ripples (I_{L1} and I_{L2}) are reduced in this mode of operation. As a result, the battery sinks power to the ultra-capacitor and the load in this situation.

2.1.3 CASE-III: Ultra-capacitor (V_{U-C}) to load (battery charges and ultra-capacitor acquittals).

When V_{UC} is connected to V_{Bat} and Vo, the ultra-capacitor provides power to the load. The battery charges at the same time. In this case, switches S_1, S_3, S_2, S_4, and S_5 will form the current path. S_2 is always in the ON position during this process.

Mode of Operation-V: Switches S_5 and S_3 are turned off, while switches S_1, S_2, and S_4 are turned on. Because of the ultra-capacitor potential, L_1 and L_2 are now energised. As a result, the inductor current increases in a linear manner. The output voltage is obtained by discharging capacitor C_1 *(See fig. 2 (e)).*

Mode of Operation-VI:

S5, S2, and S3 are turned on, but S_1 and S_4 are turned off. L_1 and L_2 inductors discharge through C_1 (*See fig. 2 (f)*). The converter's working condition results in less ripple at the output. As a result, by supplying the battery with buck operation, the ultra-capacitor acts as a primary source. The converter has increased the output voltage given to it during this time.

2.2.4 CASE IV

The ultra-capacitor and battery are powered by regenerative power (ultra-capacitor and battery in charging action).

Mode of Operation-VII:

S_1, S_3 are turned off, and S_5, S_2, S_4 are switched on. Inductors L_1 and L_2 are activated. (*See fig. 2 (g)* for more information).

Mode of Operation-IX:

The switches S_1, S_2, S_4, S_3, and S5 are all turned on, while S_5 is turned off. The load is discharged by the L_1 and L_2 inductors *(See fig. 2 (h)).* In this situation, the battery and the ultra-capacitor are charged by regenerative power created across the load. Experiment results for a variety of scenarios are shown in *figure 6* actions of a converter and in *table 2*.

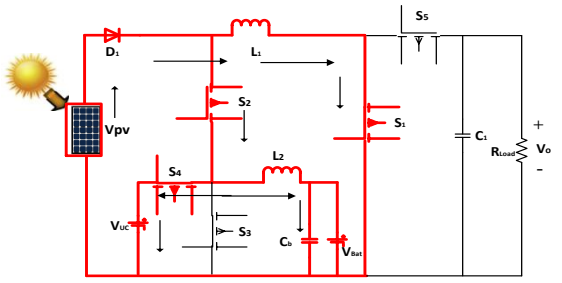

(a)

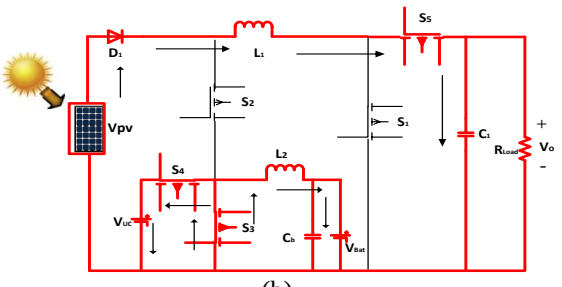

(b)

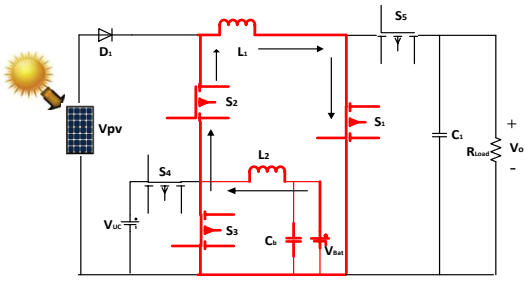

(c)

FOREX Publication
Open Access | Rapid and quality publishing
International Journal of Electrical and Electronics Research (IJEER)
Research Article | Volume 11, Issue 2 | Pages 457-464 | e-ISSN: 2347-470X

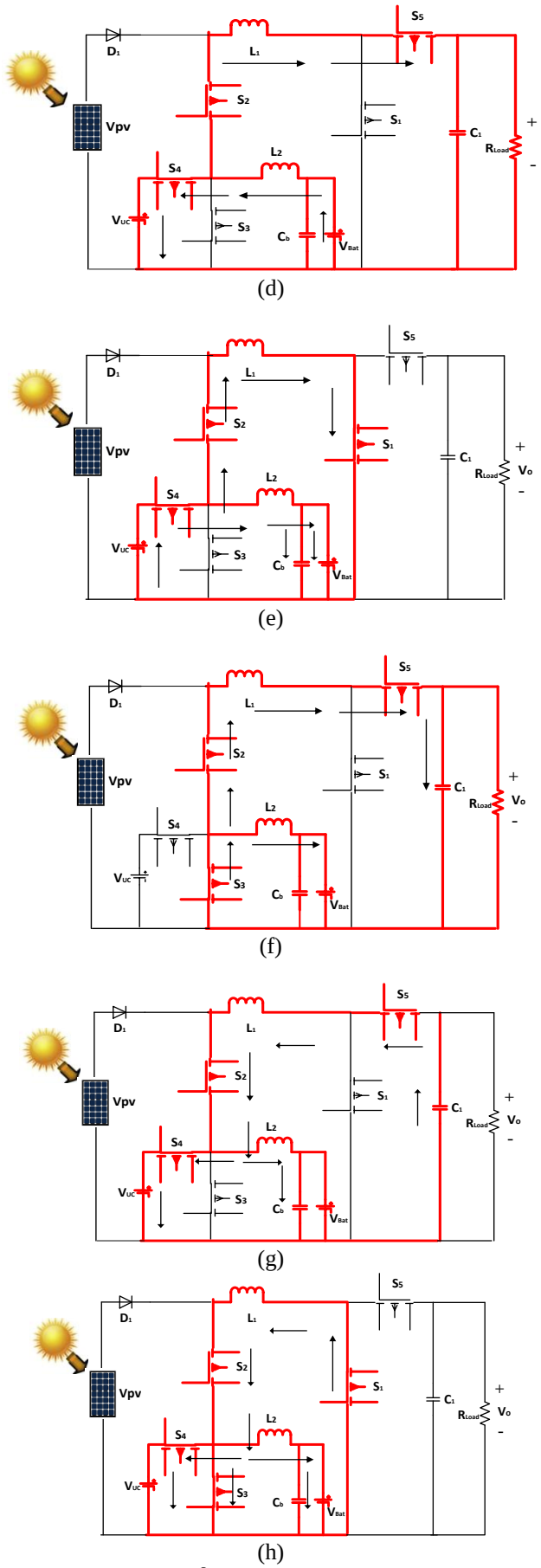

Fig.2: Operation of MIB^{3}C Case I to Case-IV [Mode of Operation (a) Mode of Operation (h)],

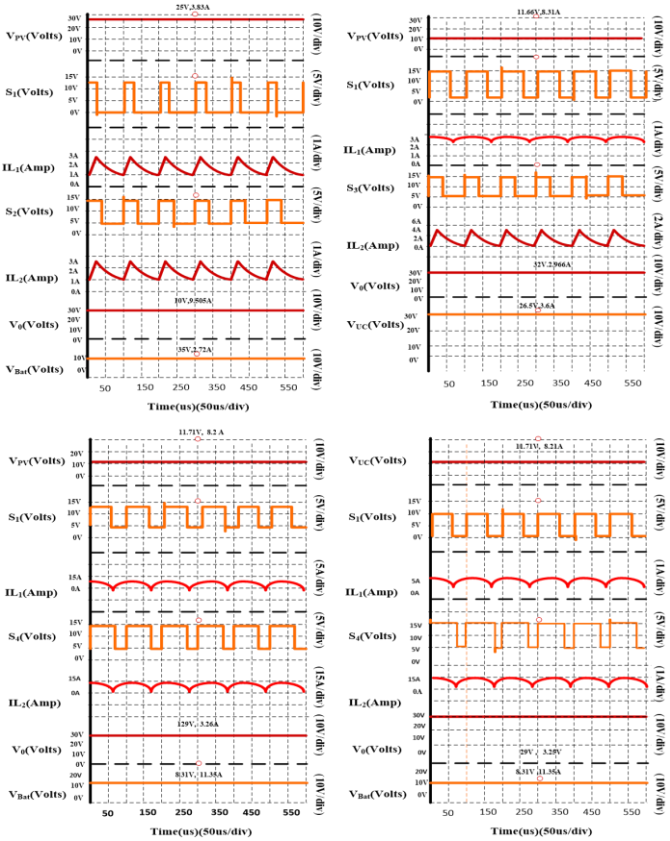

Fig.3: Switching sequence diagrams of (a) Case 1, (b) Case 2, (c) Case 3, and (d) Case 4.

For various scenarios involving the mobility of an electric vehicle, the following switching sequences have been derived from the above working principle of a four-port converter in table 2. *Figure 3* Show the under different cases converter operations with switches.

Table 2: lists the various FPB3C functioning modes for quick reference

Types of Motion	S_1	S_2	S_3	S_4	S_5	D_1
$V_{pv}>V_{batt}$, V_{u-c} uniform	ON	ON	OFF	OFF	ON	ON
	OFF	OFF	ON	ON	ON	ON
$V_{batt}>V_{u-c}$, V_{pv} uniform	ON	ON	ON	OFF	OFF	OFF
	OFF	ON	OFF	ON	ON	OFF
$V_{u-c}>V_{batt}$, Vpv uniform	ON	ON	OFF	OFF	ON	OFF
	OFF	ON	ON	ON	OFF	OFF
$V_o>V_{bat}$, V_{u-c} Braking	ON	ON	OFF	ON	ON	OFF
	OFF	ON	ON	OFF	ON	OFF
$V_{pv}=V_{batt}>V_{u-c}$ Acceleration	ON	ON	OFF	ON	OFF	OFF
	OFF	ON	OFF	ON	ON	OFF

3. EVALUATION OF A PROPOSED MULTI INPUT CONVERTER: EFFICIENCY AND LOSS ANALYSIS

A theoretical study is performed for the converter, inverter, and converter with an inverter supplied induction motor to validate these simulation findings. For this evaluation, it is assumed that

FOREX Publication
Open Access | Rapid and quality publishing
International Journal of Electrical and Electronics Research (IJEER)
Research Article | Volume 11, Issue 2 | Pages 457-464 | e-ISSN: 2347-470X

the simulation and theoretical implementation have the same parameters as:

d_1 (duty cycle of S_1) = 70% d_{11} (duty cycle of S_4) =50%
d_2 (duty cycle of S_2) = 70% d_{22} (duty cycle of S_5) =50%
d_3 (duty cycle of S_3) =50% V_{batt}=48 V_{PV}= 35V
V_{u-c}=60V

***(1) Case 1*: V_{PV}>V_{batt}, V_c, V_o**

For this situation, V_{PV} is input voltage is 35 volts. Table 3 displays the findings of a steady-state investigation of V_o, V_{batt}, and V_{u-c}.

Table 3 Summary of Simulation Results

CASES	Operation	CONVERTER OUTPUT VOLTAGE
(V_{PV}>V_{batt}, V_{u-c}, V_o).	$V_{dc-pv} = \frac{V_{dc}}{(1-d_1)}$, $V_{Batt} = d_2 V_{pv}, V_{U-C} = d_2 V_{pv}$	V_o= 115V, V_{batt}=28V
(V_{batt}>V_{u-c}, V_o)	$V_o = \frac{V_{Batt}}{(1-d_1)}, V_{U-C} = \frac{V_{Batt}}{(1-d_3)}$	V_o=155V,V_{u-c}=92V
(V_c>V_{batt},V_o)	$V_o = d_1 V_{u-c}$ $V_{Batt} = d_{22} V_{u-C},$	V_o=40V,V_{batt}=30 V

$$V_o = \frac{V_{pv}}{(1-d_1)}$$

This enhanced output allowed us to theoretically calculate the load voltage as Vo= 116.67 V.

Theoretical battery voltage and ultra-capacitor voltage were calculated using the buck result, which is $\mathbf{V_{batt} = d_2 V_{pv}}$; this gave us 25V. This means that SITO has three possible outputs: Vo = 116.67 V (boost), V_{batt} = 25 V, and V_{u-c}=25V. (BUCK)

(2) Case 2: V_{batt}>V_{u-c}, V_o

In this scenario, the input voltage, Vbatt, is 48 V, and the values for V_o and V_{u-c} in Table 3 are derived from a steady-state study.

$$V_o = \frac{V_{Batt}}{(1-d_1)}$$

(Boosted results in load) (Boosted results in load). Theoretical load voltage was calculated to be 160 V given this data.

The theoretical value of the ultra-capacitor voltage was calculated to be 96 V using the boost result of

$$V_{u-c} = \frac{V_{Batt}}{(1-d_3)}$$

This means that SIDO has two possible outputs, both of which involve V_o=160V. (BOOSTED) V_{u-c}= 96V (BOOSTED).

(3) Case 3: V_{u-c} > V_{batt}, V_o

In this scenario, the input voltage, Vbatt, is 48 volts, and the values for Vo and Vu-c in *table* 3 are derived from a steady-state study (boosted results in load). The theoretical load voltage was calculated, given this data, to be 160 V.

The theoretical value of the ultra-capacitor voltage was calculated to be 96V. Consequently, SIDO has two possible outputs: V_o = 160 V (boost) and V_{u-c}=96V. (BOOSTED).

3.1 Efficiency and Loss Analysis

The suggested multi-input bidirectional buck boost converter is much more efficient than a conventional buck boost converter with a positive output. It is possible to determine the efficiency shift of a multi-input bidirectional buck-boost converter under different operating conditions as follows:

$$\Delta\eta = \eta - \acute{\eta} = \frac{P_{output}}{P_{input} + \Delta P_{Loss}}$$

The efficiency of the converter is denoted by Δη, and the efficiency of the proposed (multi-input bidirectional buck boost) converter is considered to be η^1, where p_{output} is the output power, p_{input} is the input power, and p_{Loss} is the power loss change.

Mode-1: (Boost and Buck)

Further switching components like a diode and a MOSFET in the conduction channel between PV and load provide the extra power loss in (33).

Δp_{Loss} (Boost Mode) =P_{D1}
Δp_{Loss} (Boost Mode) =P_{S5}

The diode power (P_{D1}) and the power across the bidirectional switch (P_{S4}) are denoted below.

Mode-2: (Boost)

Between the battery and the ultra-capacitor, there are no extra switching parts, so the difference in losses can be calculated as

Δp_{Loss} (Boost) = P_{S3} + P_{S2}

P_{S1} is the power at the switch, and P_{S2} is the power at the shared switch connecting the load and the supply.

Mode-3: (Boost and Buck)

As no other components are involved in the conduction route between the loads and the battery, the variation in losses is the same as in Example Mode of Operation 2.

Δp_{Loss} (Boost) = P_{S4} + P_{S2}

Mode-4: (Buck)

Δp_{Loss} (Buck) = P_{S4} + P_{S2} + P_{S3}

4. SIMULATION RESULTS OF THE PROPOSED MULTI-INPUT CONVERTER

The power flow to the load is provided by a multi-input bidirectional buck-boost converter, which is simulated with varying input power. In the dynamic instance of electric vehicles, this suggested converter is employed to provide different sources to meet the load requirement.

The effectiveness of the suggested system is assessed here. Taking into account the real irradiation parameter, this research employs a 9.6 kW PV module produced by the Soltech firm and designated 1STH-215-P. On display in Fig.1 are the PV characteristic curves for a range of irradiance values at a fixed temperature.

FOREX Publication
Open Access | Rapid and quality publishing
International Journal of Electrical and Electronics Research (IJEER)
Research Article | Volume 11, Issue 2 | Pages 457-464 | e-ISSN: 2347-470X

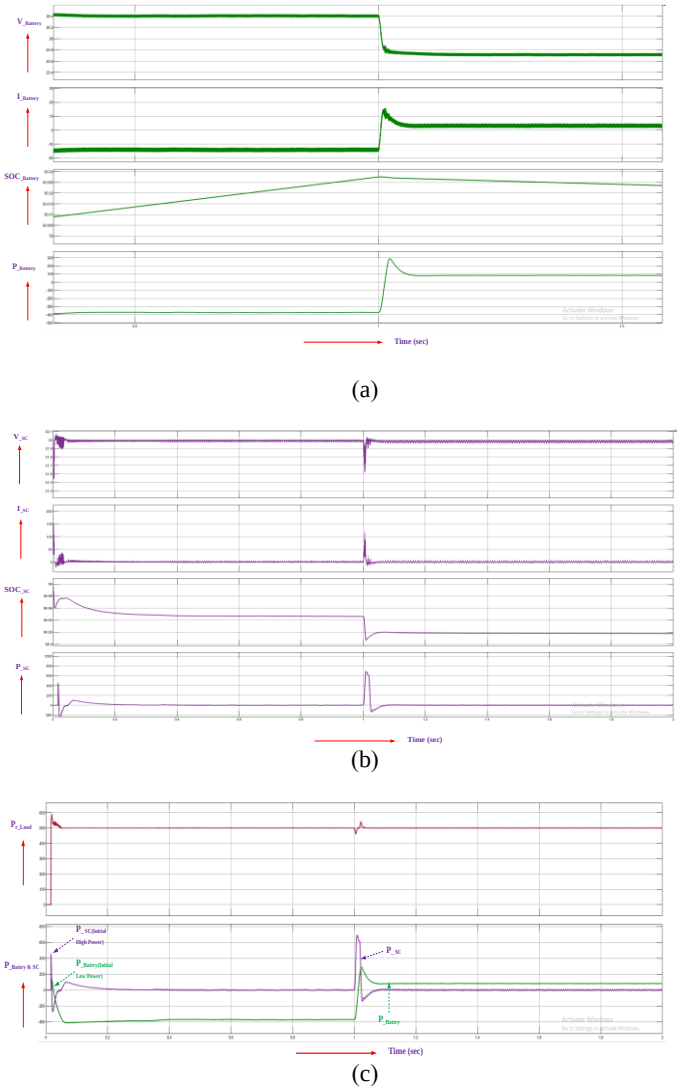

Fig.4. Simulation results of the proposed HESS applied on electric vehicles (a) Battery Output (b) Supercapacitor Output (c) Power based at Battery and Super-capacitor

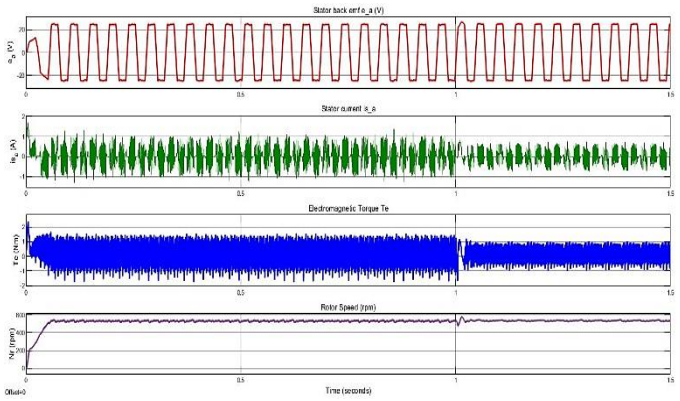

Fig.5. Steady state and starting performance of BLDC motor-drive

When the BLDC Motor is required at night, the motor-run draws a full power only from the DC bus voltage. A peak sinusoidal supply current is drawn at UPF while regulating the DC bus voltage, V_{dc} at 381.8 V. The BLDC motor run attains its full speed at 2000 rpm. The various motor-pump indices refer to back emf (e_a), stator current (i_{sa}), electromagnetic torque (T_e), speed N, are shown in *fig. 5*.

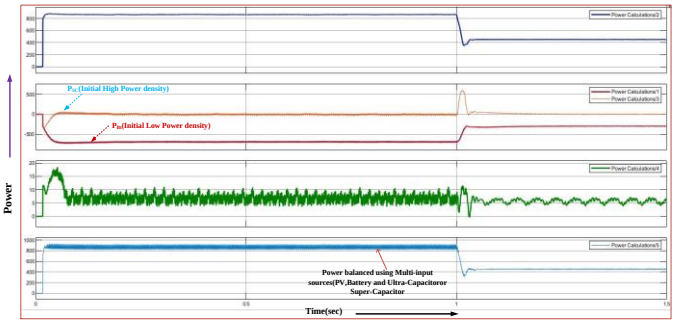

Fig.6. Using Multi input converter to send the power to load, the study state power balanced

The power flow to the load is provided by a multi-input bidirectional buck-boost converter, which is simulated with varying input power. In the dynamic instance of electric vehicles, this suggested converter is employed to provide different sources to meet the load requirement is show in *fig.6*.

5. CONCLUSIONS

In this study, a Multi-input bidirectional buck-boost converter (MIB^3C) is presented for hybrid and electric vehicle (HEV/EV) uses. The energy converter can process a wide range of inputs. Resources in one compact package, including photovoltaics, batteries, and ultra-capacitors. The complexity of the converter is decreased by the small number of components it uses, and it may provide a positive output voltage without a transformer. The converter can switch between many different modes, such as buck, boost, and buck-boost, and can handle electricity in both directions.

The continuous conduction mode (CCM) of the MIB3C has been investigated in both ideal and non-ideal situations. In addition, a PI controller is created to regulate the output voltage. To demonstrate the efficiency of the design, the converter's performance has been thoroughly evaluated over a range of operating circumstances.

MATLAB-Simulink is used for the extensive simulated research. In this analysis, the system's decreased size and weight in comparison to conventional hybrid energy storage systems is shown. Moreover, the battery's lifespan is lengthened and the ripple of output current is reduced.

6. ACKNOWLEDGMENTS

This manuscript research would not have been possible without the exceptional support of my supervisor, Dr. Manas Ranjan Nayak, who is a professor in the department of EE at BPUT, and my co-supervisor, Dr. B. Mangu, who is a professor in the department of EE at UCE-OU. Their enthusiasm, knowledge, and exacting attention to detail have been an inspiration and kept my work on track.

REFERENCES

[1] A. G. Olabi *et al.*, “Battery electric vehicles: Progress, power electronic converters, strength (S), weakness (W), opportunity

(O), and threats (T)," *International Journal of Thermofluids*, vol. 16, p. 100212, 2022.
[2] M. Dhananjaya and S. Pattnaik, "Review on multi-port DC–DC converters," *IETE Technical Review*, vol. 39, no. 3, pp. 586–599, 2022.
[3] S. Kodeeswaran, M. Nandhini Gayathri, P. Sanjeevikumar, F. IETE, and R. Peña-Alzola, "High-Power Converters and Challenges in Electric Vehicle Wireless Charging–A Review." Taylor & Francis, 2023.
[4] O. P. Jaga, R. Gupta, B. Jena, and S. GhatakChoudhuri, "Bi-directional DC/DC converters used in interfacing ESSs for RESs and EVs: a review," *IETE Technical Review*, pp. 1–37, 2022.
[5] C. Yang, Z. Lu, W. Wang, Y. Li, Y. Chen, and B. Xu, "Energy management of hybrid electric propulsion system: recent progress and a flying car perspective under three-dimensional transportation networks," *Green Energy and Intelligent Transportation*, p. 100061, 2022.
[6] S. Ditze *et al.*, "A high-efficiency high-power-density SiC-based portable charger for electric vehicles," *Electronics*, vol. 11, no. 12, p. 1818, 2022.
[7] P. Sharma, M. Sivaramakrishnaiah, B. Deepanraj, R. Saravanan, and M. V. Reddy, "A novel optimization approach for biohydrogen production using algal biomass," *International Journal of Hydrogen Energy*, 2022.
[8] M. Candon *et al.*, "Advanced multi-input system identification for next generation aircraft loads monitoring using linear regression, neural networks and deep learning," *Mechanical Systems and Signal Processing*, vol. 171, p. 108809, 2022.
[9] Z. Shi, H. Yang, and M. Dai, "The data-filtering based bias compensation recursive least squares identification for multi-input single-output systems with colored noises," *Journal of the Franklin Institute*, vol. 360, no. 7, pp. 4753–4783, 2023.
[10] L. Masike and M. N. Gitau, "A Modular Circuit Synthesis Oriented Modelling Approach for Non-Isolated DC-DC Converters in CCM," *Energies*, vol. 16, no. 3, p. 1047, 2023.
[11] K. S. Mani, M. M. Garg, and S. Dahiya, "Modeling and Control of Solar PV Integrated Boost Converter fed Battery Storage System," in *2023 Second International Conference on Electronics and Renewable Systems (ICEARS)*, IEEE, 2023, pp. 398–403.
[12] G. Gadge and Y. Pahariya, "Grey Wolf Optimization Based Energy Management Strategy for Hybrid Electrical Vehicles".
[13] Y. Bai, "Design and implementation of Silicon-Carbide-based Four-Switch Buck-Boost DCDC Converter for DC Microgrid Applications," PhD Thesis, Virginia Tech, 2023.
[14] J. R. Babu, M. R. Nayak, and B. Mangu, "A Peer Review of Hybrid Electric Vehicle Based on Step-Up Multi-input Dc-Dc Converter and renewable energy source," in *Journal of Physics: Conference Series*, IOP Publishing, 2021, p. 012041.
[15] J. R. Babu, M. R. Nayak, and B. Mangu, "Renewable Energy Applications and a Multi-Input DC-DC Converter for Hybrid Electric Vehicle Applications using Matlab/Simulink," in *2021 Innovations in Power and Advanced Computing Technologies (i-PACT)*, IEEE, 2021, pp. 1–8.
[16] J. R. Babu, M. R. Nayak, and B. Mangu, "Design And Simulation of Hybrid Electric Bicycle Powered by Solar Photovoltaics to Reduced Co2 Emissions," *Journal of Optoelectronics Laser*, vol. 41, no. 3, pp. 267–280, 2022.